# Compact N-Way Doherty Power Combiners for mm-wave 5G Transmitters

Kumaran, Anil; Nemati, Hossein Mashad ; de Vreede, Leo C.N.; Alavi, Morteza S.

**DOI**
10.1109/ISCAS48785.2022.9937619

**Publication date**
2022

**Document Version**
Final published version

**Published in**
Proceedings of the 2022 IEEE International Symposium on Circuits and Systems (ISCAS)

# Compact N-Way Doherty Power Combiners for mm-wave 5G Transmitters

Anil Kumar Kumaran*, Hossein Mashad Nemati†, Leo C.N. de Vreede*, and Morteza S. Alavi*
* Electronic Circuits and Architecture (ELCA) Research Group, Delft University of Technology
† Huawei Technologies, Sweden
Email: a.k.kumaran@tudelft.nl

2022 IEEE International Symposium on Circuits and Systems (ISCAS) | 978-1-6654-8485-5/22/$31.00 ©2022 IEEE | DOI: 10.1109/ISCAS48785.2022.9937619

***Abstract*—This paper presents a design procedure for compact lumped-element 3-/4-/5-way Doherty power combiners suitable for mm-wave 5G transmitters. Among them, the 3-way Doherty power combiner is favored due to its low complexity, compact layout, and average drain efficiency at 12 dB power back-off (PBO) when implemented using lossy lumped elements. Based on the metal stack of a 40nm CMOS process, a 3-way Doherty power combiner can provide a simulated passive efficiency of more than 60 % at 12 dB PBO and a 10 % drain-efficiency bandwidth ($BW_{\mathrm{DE10\%}}$)/3 dB power bandwidth ($BW_{\mathrm{3dB}}$) of 8/15 GHz at 30 GHz.**

***Index Terms*—Doherty, Power amplifier, Transmission line, Lumped-element, Peak-to-average power ratio.**

## I. Introduction

The millimeter-wave (mm-wave) spectrum is exploited in many upcoming applications, such as radar sensors and fifth-generation (5G) cellular networks. The latter employ spectrally efficient complex modulation schemes with high peak-to-average power ratios (PAPRs) to provide high data throughput to their users. Nevertheless, high PAPR requires a mm-wave transmitter (TX) to operate in power back-off (PBO), degrading its average efficiency (Fig. 1a).

Furthermore, 5G TXs demand sufficient radiated power to overcome the free space path loss. Accordingly, their link budget necessitates an average/peak TX power of more than 9/21 dBm, when assuming a 12 dB PAPR and 16×16 phased-array antennas [1]–[4]. Consequently, techniques like N-way Doherty are exploited to deliver the required TX power levels with decent efficiency at PBOs [5]–[9]. This paper elaborates on the systematic design of N-way Doherty power combiners to improve their efficiency at 12 dB PBO that cannot be adequately addressed using 2-way Doherty topologies.

## II. Design of N-way Doherty Networks

Figure 1b depicts N-way Doherty combiners that are inspired from [5]. In this combiner, in deep PBO, when only the main power amplifier (PA) is active, the (direct) signal path between the main PA output and overall Doherty PA output entails minimal power loss. Moreover, its efficiency is only affected by the off-state impedance of the peak-1 PA. Note that, for a symmetrical 3-/4-/5-way Doherty, the deep back-off point happens at 9.5 dB, 12 dB, and 14 dB, respectively, indicating that, at 12 dB PBO, 4-/5-way Doherty combiners are ideal candidates to enhance drain efficiency. The

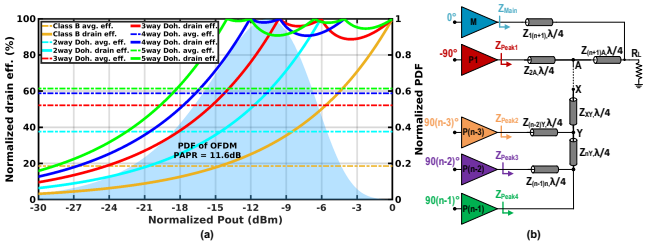


Fig. 1: (a) Normalized drain efficiency, normalized average efficiency[1], and normalized probability distribution function (PDF) of an OFDM signal vs. *Pout* for Class B and N-way Doherty, and (b) N-way Doherty structure.

following sub-sections disclose the design procedures of 3-/4-/5-way Doherty combiners and subsequently compare their performance at 12 dB PBO.

### A. 3-way Doherty PA

Figure 2a shows the 3-way Doherty structure using quarter-wavelength transmission lines (TLs). Their characteristic impedances ($Z_{14}$, $Z_{23}$, and $Z_{34}$) can be determined by analyzing the circuit's KVL and KCL at the back-off conditions ($K_2$ and $K_1$) and its full (maximum) power. At the second back-off ($K_2$), the following conditions are enforced for the voltage of the main PA ($V_{\mathrm{m@K_2}}$), the currents of the peak-1 PA ($I_{\mathrm{p1@K_2}}$), peak-2 PA ($I_{\mathrm{p2@K_2}}$) and main PA ($I_{\mathrm{m@K_2}}$):

$$\begin{aligned} V_{\mathrm{m@K_2}} &= V_{\max} = V_{\mathrm{DD}} \\ I_{\mathrm{p1@K_2}} &= I_{\mathrm{p2@K_2}} = 0,\ I_{\mathrm{m@K_2}} = I_{\mathrm{m@F}} \cdot K_2 \end{aligned} \tag{1}$$

At the first back-off point ($K_1$), the following conditions are inferred for voltages of the main PA ($V_{\mathrm{m@K_1}}$), peak-1 PA ($V_{\mathrm{p1@K_1}}$), currents of peak-2 PA ($I_{\mathrm{p2@K_1}}$), main PA ($I_{\mathrm{m@K_1}}$), and peak-1 PA ($I_{\mathrm{p1@K_1}}$):

$$\begin{aligned} V_{\mathrm{m@K_1}} &= V_{\mathrm{p1@K_1}} = V_{\max} = V_{\mathrm{DD}} \\ I_{\mathrm{p2@K_1}} &= 0,\ I_{\mathrm{m@K_1}} = I_{\mathrm{m@F}} \cdot K_1,\ I_{\mathrm{p1@K_1}} = I_{\mathrm{p1@F}} \cdot \frac{K_1 - K_2}{1 - K_2} \end{aligned} \tag{2}$$

At its maximum power, the following conditions are assumed for voltages of the main PA ($V_{\mathrm{m@F}}$), peak-1 PA ($V_{\mathrm{p1@F}}$), and peak-2 PA ($V_{\mathrm{p2@F}}$):

$$V_{\mathrm{m@F}} = V_{\mathrm{p1@F}} = V_{\mathrm{p2@F}} = V_{\max} = V_{\mathrm{DD}} \tag{3}$$

[1]Normalized drain efficiency is multiplied with the PDF of the signal and then a weighted average is performed to obtain average efficiency.

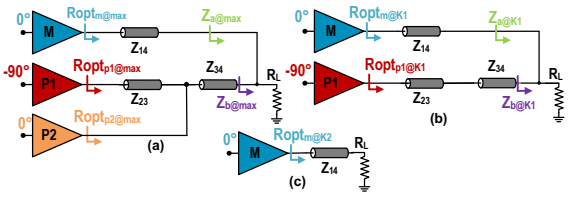


Fig. 2: 3-way Doherty network at (a) peak power, (b) back-off $K_1$, and (c) back-off $K_2$.

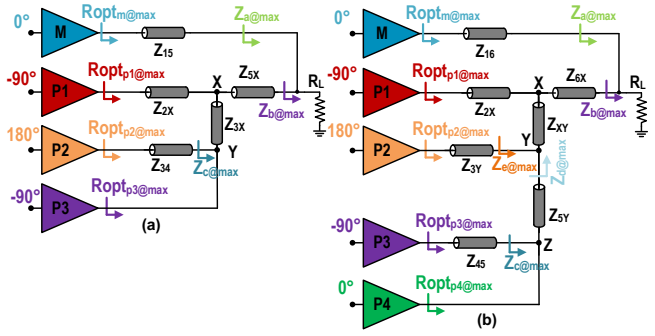


Fig. 3: (a) 4-way Doherty network at peak power and (e) 5-way Doherty network at peak power.

The back-off points can be defined as

$$K_2^2 = \frac{P_{\mathrm{m@K_2}}}{P_{\mathrm{total@max}}},\ K_1^2 = \frac{P_{\mathrm{m@K_1}} + P_{\mathrm{p1@K_1}}}{P_{\mathrm{total@max}}} \quad (4)$$
$$\text{where, } P_{\mathrm{total@max}} = P_{\mathrm{m@max}} + P_{\mathrm{p1@max}} + P_{\mathrm{p2@max}}$$

Using the Eqs. (1) to (4), we can calculate ratios of the maximum current carried by main, peak-1, and peak-2 PAs.

$$I_{\mathrm{m@max}} : I_{\mathrm{p1@max}} : I_{\mathrm{p2@max}} = [K_2 : K_1 \cdot (1-K_2) : (1-K_1)\cdot(1-K_2)] \cdot I_{\max} \quad (5)$$
$$\text{where, } I_{\max} = I_{\mathrm{m@max}} + I_{\mathrm{p1@max}} + I_{\mathrm{p2@max}}$$

The optimum impedance that a single PA requires to deliver given maximum power is:

$$Ropt_{\max} = \frac{V_{\mathrm{DD}}^2}{2 \cdot Pout_{\max}} = \frac{V_{\mathrm{DD}}}{I_{\max}} \quad (6)$$

At peak power, the optimum impedances seen by the main, peak-1, peak-2 PA are given by Eqs. (7) to (9).

$$Ropt_{\mathrm{m@max}} = \frac{V_{\mathrm{DD}}}{I_{\mathrm{m@max}}} = \frac{V_{\mathrm{DD}}}{I_{\max} \cdot K_2} = \frac{Ropt_{\max}}{K_2} \quad (7)$$

$$Ropt_{\mathrm{p1@max}} = \frac{V_{\mathrm{DD}}}{I_{\mathrm{p1@max}}} = \frac{Ropt_{\max}}{K_1 \cdot (1-K_2)} \quad (8)$$

$$Ropt_{\mathrm{p2@max}} = \frac{V_{\mathrm{DD}}}{I_{\mathrm{p2@max}}} = \frac{Ropt_{\max}}{(1-K_1)\cdot(1-K_2)} \quad (9)$$

At back-off $K_2$, the impedance seen by the main PA can be obtained by using Eqs. (1) and (7).

$$Ropt_{\mathrm{m@K_2}} = \frac{V_{\mathrm{m@K_2}}}{I_{\mathrm{m@K_2}}} = \frac{V_{\mathrm{DD}}}{I_{\mathrm{m@max}} \cdot K_2} = \frac{Ropt_{max}}{K_2^2} \quad (10)$$

From the schematic in Fig. 2c, we can get the following equation:

$$Z_{14} = \sqrt{R_{\mathrm{L}} * Ropt_{\mathrm{m@K_2}}} \quad (11)$$

The impedance seen by the main and peak1-1 PA at back-off $K_1$ is given by Eqs. (12) and (13), respectively.

$$Ropt_{\mathrm{m@K_1}} = \frac{V_{\mathrm{m@K_1}}}{I_{\mathrm{m@K_1}}} = \frac{V_{\mathrm{DD}}}{I_{\mathrm{m@max}} \cdot K_1} = \frac{Ropt_{max}}{K_1 \cdot K_2} \quad (12)$$

$$Ropt_{\mathrm{p1@K_1}} = \frac{V_{\mathrm{p1@K_1}}}{I_{\mathrm{p1@K_1}}} = \frac{Ropt_{max}}{K_1 \cdot (K_1 - K_2)} \quad (13)$$

From the schematic in Fig. 2b, we can get the following equation:

$$\frac{1}{Z_{\mathrm{a@K_1}}} + \frac{1}{Z_{\mathrm{b@K_1}}} = \frac{1}{R_{\mathrm{L}}} \quad (14)$$

The impedance seen by each PA (main, peak-1, and peak-2) is given by Eqs. (7) to (9). From the schematic in Fig. 2a, we can obtain the following equation.

$$\frac{1}{Z_{\mathrm{a@max}}} + \frac{1}{Z_{\mathrm{b@max}}} = \frac{1}{R_{\mathrm{L}}} \quad (15)$$

In this regard, from the three equations (Eqs. (11), (14), and (15)), the generalized equations for the characteristic impedance of the three TLs ($Z_{14}, Z_{23}$, and $Z_{34}$) can be calculated in terms of $Ropt_{\max}$, $V_{\mathrm{DD}}$, $R_{\mathrm{L}}$, $K_1$ and $K_2$ (Eq. (16)).

$$Z_{14} = \frac{\sqrt{R_{\mathrm{L}} \cdot Ropt_{\max}}}{K_2}, Z_{23} = \frac{Ropt_{\max}}{K_1 \cdot (1-K_2)}$$
$$Z_{34} = \frac{\sqrt{R_{\mathrm{L}} \cdot Ropt_{\max}}}{(1-K_2)} \quad (16)$$

### B. 4-way Doherty PA

Figure 3a depicts the 4-way Doherty network using quarter-wavelength TLs. We can calculate the ratios of maximum current carried by the main, peak-1, peak-2, and peak-3 PAs by analyzing the circuit's KVL and KCL conditions at the back-off points ($K_1$, $K_2$, and $K_3$) and the full power similar to its 3-way Doherty counterpart.

$$I_{\mathrm{m@max}} : I_{\mathrm{p1@max}} : I_{\mathrm{p2@max}} : I_{\mathrm{p3@max}} = [K_3 : K_2 \cdot (1-K_3) : (1-K_2)\cdot(K_1-K_3) : (1-K_1)\cdot(1-K_2)] \cdot I_{\max} \quad (17)$$

The characteristic impedance of its five TLs ($Z_{15}$, $Z_{2X}$, $Z_{3X}$, $Z_{5X}$, and $Z_{34}$) can be calculated similarly to the 3-way Doherty network by analyzing the circuit at the back-off conditions ($K_1$, $K_2$, and $K_3$) and maximum power, which gives four equations. Since the current delivered by peak-2 and peak-3 at the peak power is $(1-K_2)\cdot(K_1-K_3)\cdot I_{\max}$ and $(1-K_1)\cdot(1-K_2)\cdot I_{\max}$, respectively (Eq. (17)), we can calculate the ratio between the impedances $Z_{\mathrm{c@max}}$ and $Ropt_{\mathrm{p3@max}}$ (Eq. (18)) by applying KCL at node Y (see Fig. 3a), providing the 5$^{\mathrm{th}}$ equation. In this context, solving the five equations, we find that $Z_{2X}$, $Z_{3X}$, and $Z_{5X}$ have dependant relation, giving the designer one degree of freedom in choosing the characteristic impedance of either $Z_{2X}/Z_{3X}/Z_{5X}$. The generalized characteristic impedance of the TLs can be calculated using $Ropt_{\max}$, $V_{\mathrm{DD}}$, $R_{\mathrm{L}}$, $K_1$, $K_2$, and $K_3$ (Eq. (19)).

$$Z_{\mathrm{c@max}} = Ropt_{\mathrm{p3@max}} \cdot \frac{1-K_1}{K_1-K_3}$$
$$Z_{34} = \sqrt{Z_{\mathrm{c@max}} \cdot Ropt_{\mathrm{p2@max}}} = \frac{Ropt_{\max}}{(1-K_2)\cdot(K_1-K_3)} \quad (18)$$

$$Z_{15}=\frac{\sqrt{R_L\cdot Ropt_{max}}}{K_3},\ Z_{2X}=\frac{\sqrt{R_L\cdot Ropt_{max}}\cdot Z_{5x}}{K_2\cdot R_L}$$
$$Z_{3X}=\frac{\sqrt{R_L\cdot Ropt_{max}}\cdot Z_{5x}}{(1-K_2)\cdot R_L},\ Z_{34}=\frac{Ropt_{max}}{(1-K_2)\cdot(K_1-K_3)} \quad (19)$$

### C. 5-way Doherty PA

Figure 3b exhibits the 5-way Doherty network using quarter-wavelength TLs. We can calculate the ratios of maximum current carried by the main, peak-1, peak-2, peak-3, and peak-4 PAs by analyzing the circuits' KVL and KCL at its back-off points ($K_1$, $K_2$, $K_3$, and $K_4$) and the full power similar to its 3-way Doherty companion.

$$I_{m@max}:I_{p1@max}:I_{p2@max}:I_{p3@max}:I_{p4@max}=$$
$$[K_4:K_3\cdot(1-K_4):(1-K_3)\cdot(K_2-K_4):$$
$$(K_1-K_3)\cdot(1-K_2):(1-K_3)\cdot(1+K_4-2K_2)]\cdot I_{max} \quad (20)$$

The characteristic impedance of its seven TLs ($Z_{16}$, $Z_{2X}$, $Z_{6X}$, $Z_{XY}$, $Z_{3Y}$, $Z_{5Y}$ and $Z_{45}$) can be calculated by analyzing the circuit at the back-off conditions ($K_1$, $K_2$, $K_3$, and $K_4$) and maximum power, giving five equations. The 5$^{th}$ and 6$^{th}$ equations can be obtained by applying KCL at node Y and Z at peak power similarly to its 4-way Doherty counterpart (Fig. 3b). In this approach, by solving the seven equations, we find that $Z_{2X}$, $Z_{3Y}$, $Z_{5Y}$, $Z_{XY}$, and $Z_{6X}$ have a dependent relation, providing the designer two degrees of freedom in choosing the characteristic impedance of two TLs among $Z_{2X}$, $Z_{3Y}$, $Z_{5Y}$, $Z_{XY}$, and $Z_{6X}$. The generalized characteristic impedance of the TLs can be calculated using $Ropt_{max}$, $V_{DD}$, $R_L$, $K_1$, $K_2$, $K_3$, and $K_4$ (Eq. (21)).

$$Z_{16}=\frac{\sqrt{R_L\cdot Ropt_{max}}}{K_4},\ Z_{2X}=\frac{\sqrt{R_L\cdot Ropt_{max}}\cdot Z_{6x}}{K_3\cdot R_L}$$
$$Z_{3Y}=\frac{\sqrt{K_3\cdot R_L\cdot Ropt_{max}\cdot(K_2-K_3)}\cdot(1-K_3)\cdot Z_{XY}}{K_3\cdot Z_{6X}\cdot(K_3\cdot K_2-K_3\cdot K_4-K_2+K_4)}$$
$$Z_{5Y}=$$
$$\frac{\sqrt{K_3\cdot R_L\cdot Ropt_{max}\cdot(K_2-K_3)}\cdot(1-K_3)\cdot Z_{XY}}{K_3\cdot Z_{6X}\cdot((2+K_4-3\cdot K2)\cdot K_3+(K_1+2)\cdot K_2-K_1-K_4-1)}$$
$$Z_{45}=\frac{Ropt_{max}}{(1-K_2)\cdot(K_1-K_3)} \quad (21)$$

The equations for symmetrical 3-/4-/5-way Doherty with their associated back-off points are presented in Table I.

## III. Analysis

In this section, we design the symmetrical 3-/4-/5-way Doherty PAs that can deliver a $Pout_{max}$ of 22 dBm to a load ($R_L$) of 25 Ω (for a single-ended Doherty PA) with a $V_{DD}$ of 1 V using equations in Table I. The TLs can be modeled using a high-pass lumped component model (Fig. 4a) at the center frequency of 30 GHz (Fig. 4b/c/d). Since the high-pass lumped component model allows a DC feed for each PA, a differential implementation is straightforward. As exhibited, moving from N to N+1 Doherty, the number of TL elements increases by 2. Similarly, in the case of lumped components, inductors and capacitors increase by 2.

The PAs are modeled as an ideal current source in ADS to analyze their output power (*Pout*) and drain efficiency (DE) of

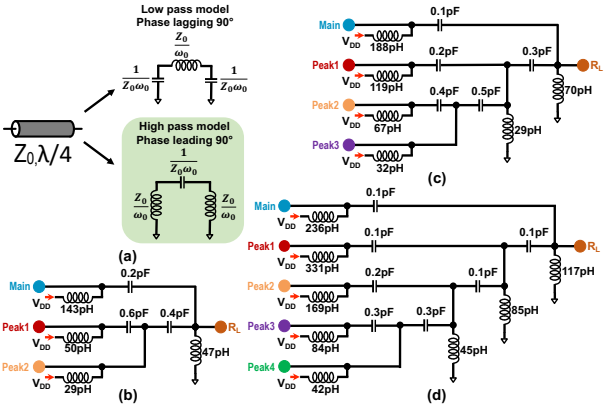


Fig. 4: (a) High-pass and low-pass model of TL, (b) 3-way Doherty network, (c) 4-way Doherty network, and (d) 5-way Doherty network using lumped components.

TABLE I: COMPARISON OF 3-/4-/5-WAY DOHERTY COMBINERS.

| Parameters | 3-way Doherty | 4-way Doherty | 5-way Doherty |
|---|---|---|---|
| **Transmission lines** | 3 | 5 | 7 |
| **Lumped components** | Ind-4 & Cap-3 | Ind-6 & Cap-5 | Ind-8 & Cap-7 |
| **Degrees of freedom** | 0 | 1 | 2 |
| **$Pout_{max}$ per PA*** (dBm) | $Pout_{max}-10\cdot\log(3)$ = 17.2 | $Pout_{max}-10\cdot\log(4)$ = 16 | $Pout_{max}-10\cdot\log(5)$ 15 |
| **Back-off points*** | $K_1$=0.5, $K_2$=0.333 | $K_1$=0.625, $K_2$=0.333, $K_3$=0.25 | $K_1$=0.625, $K_2$=0.467, $K_3$=0.25, $K_4$=0.2 |
| **Ropt for each PA @max power*** (Ω) | $\frac{Ropt_{max}}{K2}$ = 9.6 | $\frac{Ropt_{max}}{K3}$ = 12.7 | $\frac{Ropt_{max}}{K4}$ = 15.9 |
| **$Z_0$ of transmission lines*** (Ω) | $Z_{14}=3\cdot\sqrt{R_L\cdot Ropt_{max}}$<br>$Z_{23}=3\cdot Ropt_{max}$<br>$Z_{34}=\frac{3\cdot\sqrt{R_L\cdot Ropt_{max}}}{2}$ | $Z_{15}=4\cdot\sqrt{R_L\cdot Ropt_{max}}$<br>$Z_{2X}=\frac{3\cdot\sqrt{R_L\cdot Ropt_{max}\cdot Z_{5x}}}{R_L}$<br>$Z_{3X}=\frac{3\cdot\sqrt{R_L\cdot Ropt_{max}}\cdot Z_{5x}}{2\cdot R_L}$<br>$Z_{34}=4\cdot Ropt_{max}$<br>$Z_{5X}$ - user-defined | $Z_{16}=5\cdot\sqrt{R_L\cdot Ropt_{max}}$<br>$Z_{2X}=\frac{4\cdot\sqrt{R_L\cdot Ropt_{max}\cdot Z_{6X}}}{R_L}$<br>$Z_{3Y}=\frac{3.5\cdot\sqrt{R_L\cdot Ropt_{max}}\cdot Z_{XY}}{Z_{6X}}$<br>$Z_{5Y}=\frac{3.5\cdot\sqrt{R_L\cdot Ropt_{max}}\cdot Z_{XY}}{2\cdot Z_{6X}}$<br>$Z_{45}=5\cdot Ropt_{max}$<br>$Z_{6X}$ & $Z_{XY}$ - user-defined |

* To generate $Pout_{max}$ = 22 dBm with $V_{DD}$ = 1 V in the symmetrical Doherty for a load ($R_L$) of 25 Ω

the 3-/4-/5-way Doherty network at peak and back-off power levels at the mm-wave band centered around 30 GHz. According to Fig. 5a, the designed 3-/4-/5-way Doherty network using lossless lumped components obtain 3/4/5 DE peaks of 78.5 % (ideal Class B) as expected while delivering $Pout_{max}$=22 dBm. The peak DE can be improved further by utilizing class J or continuous class F PAs [10] [11]. Subsequently, the 3-/4-/5-way Doherty are modeled with lossy elements assuming quality factors (QFs) of 15/25 for the inductors/capacitors, respectively, and simulated with an ideal PA to capture its *Pout* and DE at the mm-wave band centered around 30 GHz. According to Fig. 5a, the 5-way Doherty achieves a lower peak DE and $Pout_{max}$ since the number of lumped components in the power combiner is higher, entailing higher loss.

At 12 dB back-off (Fig. 5b), the 3-way Doherty has the highest *Pout* since only the main PA is active. Nevertheless, the 5-way Doherty has the best DE performance because load modulation has already been started at $K_4$=0.2 and $K_3$=0.25. The 3-/4-way Doherty PAs have similar performance at 30 GHz because, in the 3-way Doherty, the load modulation has not been started, and in the 4-way Doherty, load modulation has just been started (peak-1 PA turning on at $K_3$=0.25). On the other hand, the bandwidth at which DE drops by 10 % ($BW_{DE10\%}$) and 3 dB power bandwidth ($BW_{3dB}$) is maximum for 5-way Doherty followed by 3-/4-way Doherty at

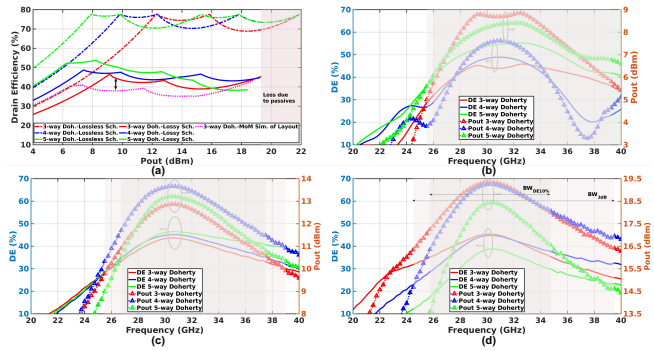


Fig. 5: (a) DE vs. *Pout* for 3-/4-/5-way Doherty at 30 GHz using lossless and lossy lumped components, (b) DE and *Pout* vs. frequency for 3-/4-/5-way Doherty at PBO 12 dB, (c) PBO 6 dB, and (d) full power using inductors/capacitors of quality factors of 15/25, respectively.

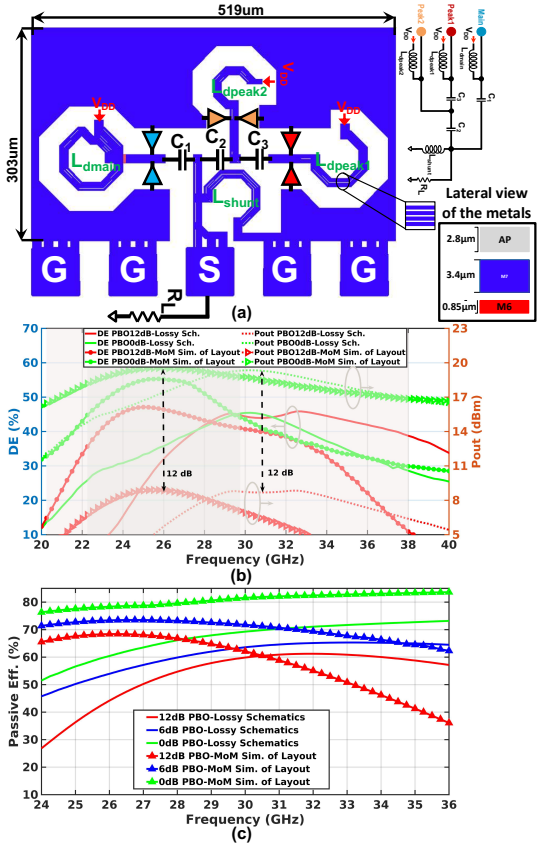


Fig. 6: (a) Layout of 3-way Doherty (b) DE vs. frequency for 3-way Doherty at 12 dB PBO and maximum power, and (c) PE vs. frequency for 3-way Doherty at 12 dB PBO, 6 dB PBO and maximum power using inductors/capacitors of quality factors of 15/25, respectively, and momentum simulation of the layout.

12 dB back-off ($BW_{\mathrm{DE10\%}}/BW_{\mathrm{3dB}}$ of 3-way Doherty is shaded in green/red in Fig. 5b/c/d). Additionally, at 6 dB back-off (Fig. 5c), DE performance is similar in all cases. Nonetheless, *Pout* is the highest for 4-way Doherty because its peak-3 PA has not turned on yet. However, in the 3-way Doherty, its three PAs are on, leading to higher current, higher losses, and thus lower *Pout*. In contrast, in the 5-way Doherty, although the related current is lower, the number of lumped components operating in the network is higher, giving rise to the higher loss, and thus, lower *Pout*. Their $BW_{\mathrm{DE10\%}}/BW_{\mathrm{3dB}}$ at 6 dB back-off is comparable. Figure 5d illustrates that DE and *Pout* at maximum power are lower for 5-way Doherty due to the higher number of lumped elements, entailing higher losses. These simulation results also indicate that DE and *Pout* at full power are similar for 3-/4-way Doherty. Moreover, $BW_{\mathrm{DE10\%}}$ is lower at maximum power than the back-off points for all cases. It also reveals that $BW_{\mathrm{DE10\%}}$ at full power reduces as we move from 3- to 5-way Doherty (Fig. 5b/c/d).

Consequently, the 3-way Doherty is the best choice for implementing PA in mm-wave frequency bands. Moreover, employing a 4-way Doherty and beyond cannot deliver the required maximum power due to the higher insertion loss of lumped-element power combiner, although it requires lower impedance transformation. Furthermore, the performance of 3-way Doherty is comparable with the 4-way Doherty at 12 dB back-off and has better performance at peak power. Finally, it only consists of three quarter-wavelength TLs, giving rise to minimal lumped-element high-pass equivalent TLs and thus a compact power combiner.

The proposed 3-way Doherty structure is laid out in an LP 40nm CMOS process (Fig. 6a) with a size of $519 \times 303\,\mu m^2$. In this regard, QF of the spiral/slab inductors is increased more than twofold using parallel slot lines of minimum width than utilizing one thick line of the required width, as shown in Fig. 6a. Since the signal travels at the surface due to the skin effect, splitting the lines increases surface area, reducing resistance and increasing Q [12]. The ADS (Momentum) simulation results of the layout are depicted in Fig. 6b/c, which indicates at most 10 % deviation in passive efficiency (PE) from the assumed lossy network. Also, the proposed layout reaches PE of 60 % at 12 dB PBO while operating at 30 GHz. The center frequency has shifted to 26 GHz due to the addition of the ground plane, which affects the related inductance of the network. This arrangement can be tuned if necessary. Moreover, using an ideal PA, the proposed design achieves a peak RF output power/drain efficiency of more than 20dBm/55%, respectively, and its $BW_{\mathrm{DE10\%}}/BW_{\mathrm{3dB}}$ is 8/15 GHz, shaded green/red, respectively (Fig. 6b).

## IV. Conclusion

This paper elaborates on the systemic design procedure for 3-/4-/5-way Doherty PAs using transmission lines and lumped-element that can be extended to an N-way Doherty network. Accordingly, these power combiners are designed and compared using lossless and lossy components with quality factors of 15/25 for inductors/capacitors at 30 GHz while their PAs are modeled as ideal current sources. According to these analyses, using a realistic Q factor for the inductors, we conclude that the 3-way Doherty network is the best candidate at mm-wave frequency bands since it has only four inductors and three capacitors, leading to less complexity, compact layout, and demonstrates a performance comparable to that of 4-way Doherty at 12 dB back-off. Finally, the 3-way Doherty is laid out in a 40nm CMOS process metal stack, achieving a simulated peak RF output power/drain efficiency of 20 dBm/55 % and $BW_{\mathrm{DE10\%}}/BW_{\mathrm{3dB}}$ of 8/15 GHz at 30 GHz.

## REFERENCES


[1] M. Pashaeifar *et al.*, "A 24-to-30 GHz Double-Quadrature Direct-Upconversion Transmitter with Mutual-Coupling-Resilient Series-Doherty Balanced PA for 5G MIMO Arrays," in *2021 IEEE Int. Solid-State Circuits Conference (ISSCC)*, 2021, pp. 223–225.

[2] I. Ahmed *et al.*, "A Survey on Hybrid Beamforming Techniques in 5G: Architecture and System Model Perspectives," *IEEE Communications Surveys Tutorials*, vol. 20, no. 4, pp. 3060–3097, 2018.

[3] S. A. Busari *et al.*, "Millimeter-Wave Massive MIMO Communication for Future Wireless Systems: A Survey," *IEEE Communications Surveys Tutorials*, vol. 20, no. 2, pp. 836–869, 2018.

[4] T. Tuovinen *et al.*, "Analyzing 5G RF System Performance and Relation to Link Budget for Directive MIMO," *IEEE Transactions on Antennas and Propagation*, vol. 65, no. 12, pp. 6636–6645, 2017.

[5] M. Beikmirza *et al.*, "A 4-Way Doherty Digital Transmitter Featuring 50%-LO Signed IQ Interleave Upconversion with more than 27dBm Peak Power and 40% Drain Efficiency at 10dB Power Back-Off Operating in the 5GHz Band," in *2021 IEEE Int. Solid- State Circuits Conference (ISSCC)*, 2021, pp. 92–94.

[6] E. Kaymaksut *et al.*, "Transformer-Based Doherty Power Amplifiers for mm-Wave Applications in 40-nm CMOS," *IEEE Transactions on Microwave Theory and Techniques*, vol. 63, no. 4, pp. 1186–1192, 2015.

[7] F. Wang *et al.*, "A Super-Resolution Mixed-Signal Doherty Power Amplifier for Simultaneous Linearity and Efficiency Enhancement," *IEEE Journal of Solid-State Circuits*, vol. 54, no. 12, pp. 3421–3436, 2019.

[8] F. Wang and H. Wang, "A 24-to-30GHz Watt-Level Broadband Linear Doherty Power Amplifier with Multi-Primary Distributed-Active-Transformer Power-Combining Supporting 5G NR FR2 64-QAM with 19dBm Average Pout and 19% Average PAE," in *2020 IEEE Int. Solid-State Circuits Conference - (ISSCC)*, 2020, pp. 362–364.

[9] M. Pashaeifar *et al.*, "A 24-to-32GHz series-Doherty PA with two-step impedance inverting power combiner achieving 20.4dBm Psat and 38%/34% PAE at Psat/6dB PBO for 5G applications," in *2021 IEEE Asian Solid-State Circuits Conference (A-SSCC)*, 2021, pp. 1–3.

[10] M. S. Alavi *et al.*, "Efficient LDMOS device operation for envelope tracking amplifiers through second harmonic manipulation," in *2011 IEEE MTT-S Int. Microwave Symposium (IMS)*, 2011, pp. 1–4.

[11] A. K. Kumaran *et al.*, "On-Chip Output Stage Design for a Continuous Class-F Power Amplifier," in *2021 IEEE Int. Symposium on Circuits and Systems (ISCAS)*, 2021, pp. 1–5.

[12] H. Gao *et al.*, "A 48–61 GHz LNA in 40-nm CMOS with 3.6 dB minimum NF employing a metal slotting method," in *2016 IEEE Radio Frequency Integrated Circuits Symposium (RFIC)*, 2016, pp. 154–157.